A 2V CMOS Capacitorless Current-Tunable All-Pass Filter using Current Mirrors

Banlue Srisuchinwong and Adisorn Leelasantitham
Electrical Engineering Program, Sirindhorn International Institute of Technology,
Thammasat University, P.O.Box 22, Thammasat Rangsit Post Office, Patumthani 12121, Thailand,
Tel : (+66 2) 986 9009, Fax : (+66 2) 986 9112, 986 9113, banlue@siit.tu.ac.th

Abstract

A 2V CMOS capacitorless current-tunable all-pass filter using current mirrors is presented through the use of the MOS internal capacitances. The frequency f_o where the magnitude and phase shift of the transfer function are approximately 0 dB and –90°, respectively, is tunable through the bias current. The maximum useful f_o is in excess of 700MHz depending on the internal parameters.

1. Introduction

All-pass filters are utilised in many applications such as in sinusoidal quadrature oscillators. Most techniques of integrable all-pass filters employ relatively large external capacitors and therefore the operating frequencies are not relatively high [1-4]. Recently, capacitorless techniques have exploited not only the paracitic capacitances of BJTs for high-frequency all-pass filters [5] or integrators [6], but also the internal capacitances of MOS for high-frequency bandpass filters [7] or switched-current circuits [8].

In this paper, a 2V high-frequency CMOS capacitorless current-tunable all-pass filter using current mirrors is presented through the use of the MOS internal capacitances. The frequency f_o where the magnitude and phase shift of the transfer function are approximately 0 dB and –90°, respectively, is tunable through the bias current. The maximum useful f_o is in excess of 700 MHz depending on the internal parameters.

2. Circuit Descriptions

Figure 1 shows the circuit of the CMOS capacitorless current-tunable all-pass filter. The circuit consists of current mirrors formed by five NMOS transistors Q1 to Q5 and three current sources I, 2I and 4I. Q1 to Q3 are identical and the aspect ratios are W/L. The aspect ratios of Q4 and Q5 are separated into two cases. In the first case, the ratios are 16W/L and 32W/L respectively. In the second case, the ratios are 2W/L and 4W/L, respectively. The small signal input current i_{in} is applied to the drain of Q1 and the resulting small signal output current i_o is taken from the drain of Q5.

3. Ideal Analysis

For a MOS transistor, the unity current gain frequency ω_T is equal to g_m/C where $C = (C_{gs} + C_{gd} + C_{gb})$ [9] and $g_m = (2I)/(V_{GS} - V_T)$. C_{gs}, C_{gd} and C_{gb} are the MOS internal capacitances. The subscripts g, s, d and b stand for gate, source, drain and body of a MOS transistor. V_{GS} is the gate source voltage. V_T is the usual threshold voltage and I is the bias current. Referring to Figure 1, the small signal current i_x yields

$$i_x = \frac{i_{in}}{1+s\tau_a} \tag{1}$$

where the time constant $\tau_a = C_a/g_{m1}$, $C_a = (C_{gs} + C_{gb})_1 + (C_{gs} + C_{gd} + C_{gb})_2 + (C_{gs} + C_{gd} + C_{gb})_3$ and $g_{m1} = (2I) / (V_{GS1} - V_T)$. The subscripts 1 to 3 refer to Q1 to Q3. Similarly, the small signal current i_y is equal to

$$i_y = \frac{2i_x}{1+s\tau_b} \tag{2}$$

where the time constant $\tau_b = C_b/g_{m4}$, $C_b = (C_{gs} + C_{gb})_4 + (C_{gs} + C_{gd} + C_{gb})_5$ and $g_{m4} = (2I) / (V_{GS4} - V_T)$. The subscripts 4 and 5 refer to Q4 and Q5. In addition, $i_y = i_o + i_x$. Therefore, the transfer function $\mathbf{T(s)} = i_o/i_{in}$ yields

$$\mathbf{T(s)} = \frac{(1 - s\tau_b)}{(1 + s\tau_a)(1 + s\tau_b)} \qquad (3)$$

For sinusoidal input, the magnitude M and phase shift ϕ of equation (3) are of the form

$$M = -20\log\sqrt{1 + \omega^2\tau_a^2} \qquad (4)$$

$$\phi = \tan^{-1}(-\omega\tau_b) - \tan^{-1}(\omega\tau_b) - \tan^{-1}(\omega\tau_a) \qquad (5)$$

Equation (3) can be considered in two cases. In the first case for $\tau_a << \tau_b$, equation (3) is reduced to a first-order all-pass filter of the form

$$\mathbf{T(s)} \cong \frac{(1 - s\tau_b)}{(1 + s\tau_b)} \qquad (6)$$

In this case, the magnitude and phase shift of equation (6) are 0 dB and –90°, respectively, at the frequency $\omega = \omega_1$ for

$$\omega_1 = 1/\tau_b = g_{m4}/ C_b = (2I) / [(V_{GS4} - V_T)\, C_b\,] \qquad (7)$$

In the second case for $\tau_a < \tau_b$, equation (3) may be approximated as an all-pass filter where M described in (4) approaches 0 dB at ϕ = –90° and at $\omega = \omega_o = h\omega_1$ for

$$h = \sqrt{\frac{\tau_b}{2\tau_a + \tau_b}} \qquad (8)$$

It can be seen from (7) and (8) that ω_o and ω_1 are tunable through the bias current I and hence the name "current-tunable".

4. Simulation Results

The performance of the circuit shown in Figure 1 has been simulated using SPICE and all transistors are in saturation mode. The CMOS transistors are modeled by Alcatel Mietec 0.5 μm CMOS C05MD Technology from EUROPRACTICE. The width W and length L are equal to 0.5 μm. The supply voltage V_{CC} = 2 V and V_T = 0.68 V. Table 1 shows the internal capacitances of Q1 to Q5. Table 2 shows values of τ_a and τ_b at I = 20 μA.

Table 1.Internal capacitances of Q1 to Q5

	Ratios	C_{gs} (F.)	C_{gd} (F.)	C_{gb} (F.)
Q1, Q2, Q3	W/L	1×10^{-15}	1×10^{-16}	3×10^{-16}
Q4	2W/L	2×10^{-15}	2×10^{-16}	6×10^{-16}
Q5	4W/L	4×10^{-15}	4×10^{-16}	12×10^{-16}
Q4	16W/L	16×10^{-15}	16×10^{-16}	48×10^{-16}
Q5	32W/L	32×10^{-15}	32×10^{-16}	96×10^{-16}

Table 2. Values of τ_a and τ_b at I = 20 μA.

	Ratios	current (μA)	V_{GS} (V)	τ_a (10^{-11}s)	τ_b (10^{-11}s)
Q1, Q2, Q3	W/L	I = 20	1.14	4.715	-
Q4	2W/L	I = 20	1.01	-	6.663
Q5	4W/L	2I = 40	1.01	-	
Q4	16W/L	I = 20	0.79	-	18.830
Q5	32W/L	2I = 40	0.79	-	

Let the aspect ratios of Q4 and Q5 be 16W/L and 32W/L, respectively, and represent an approximated example of the all-pass filters described in the first case where $\tau_a << \tau_b$. In this case, h = 0.81 where M and ϕ are –0.1 dB and –90°, respectively. For such a case, Figure 2 depicts $f_o = \omega_o/(2\pi)$ and M at ϕ = –90° versus I using dotted and solid lines for the expected and simulated results, respectively.

On the other hand, let the aspect ratio of Q4 and Q5 be 2W/L and 4W/L, respectively, and represent an example of the approximated all-pass filter described in the second case where $\tau_a < \tau_b$. In this case, h = 0.64 where M and ϕ are –0.7 dB and –90°, respectively. For such a case, Figure 3 shows $f_o = \omega_o/(2\pi)$ and M at ϕ = –90° versus I using dotted and solid lines for the expected and simulated results, respectively. It can be seen from Figures 2 and 3 that the expected and simulated results are in resonably good fits.

Figure 4 shows the magnitude (dB) and phase shift (degrees) of (6) and (3) versus frequency (Hz) at bias current I = 20 μA and 50 μA for the first case ($\tau_a << \tau_b$) and the second case ($\tau_a < \tau_b$), respectively. It can be seen from Figure 4 that, the frequency (f_o) at phase shift of –90° for the first case and the second case are approximately 700 MHz and 2 GHz, respectively, whilst the corresponding magnitude are approximately –0.1 dB and –0.7 dB, respectively.

5. Discussions

It can be seen from Figures 2 and 3 that f_o of the first case ($\tau_a << \tau_b$) is lower than f_o of the second case ($\tau_a < \tau_b$), and the maximum useful f_o are approximately 700 MHz and 2 GHz, respectively. On the other hand, M of the first case is better than M of the second case but may be further amplified by a wide band amplifier for further use. For applications at high frequencies, the second case ($\tau_a < \tau_b$) can be considered more attractive than the first case ($\tau_a << \tau_b$) in terms of higher value of f_o if τ_a of the two cases are the same.

Under small-signal operation and ideal current sources, the input and output impedances of the circuit shown in Figure 1 are $Z_{in} = (1/g_{m1}) / (1+s\tau_a)$ and $Z_{out} \cong r_o/2$, respectively, where r_o is a finite resistance of MOS between drain and source occurring from the effect of channel-length modulation. The input impedance is a typical value of approximately $1/g_{m1}$ at low frequency. The output impedance can be improved through the use of conventional cascode techniques with an expense of lower f_o due to additional internal capacitances.

The ideal current sources shown in Figure 1 can be realized through practical PMOS current sources but the f_o and magnitude (dB) at –90 degrees versus I may slightly be decreased because of additional capacitance C_{ds} from a PMOS transistor. However, the source is connected to the body and therefore $C_{ds} \cong C_{db}$ where C_{db} can usually be neglected [10].

6. Conclusions

A 2V CMOS capacitorless current-tunable all-pass filter using current mirrors has been presented through the use of the MOS internal capacitances. The frequency f_o where the magnitude and phase shift of the transfer function are approximately 0 dB and –90°, respectively, is tunable through the bias current. The maximum useful f_o is in excess of 700 MHz depending on the internal parameters.

7. Acknowledgements

The authors are grateful to The Royal Golden Jubilee PhD Program for the financial supports.

8. References

[1] Pookaiyaudom, S. and Samootrut, K., Current-Mirror Phase-Shifter Oscillator Electron. Lett., vol. 23, no.1, January, pp. 21-23, 1987.

[2] Bult, K. and Walling, A., A CMOS Analog Continuous-Time Delay Line with Adaptive Delay-Time Control, IEEE J. of Solid-State Circuits, vol. 23, no. 3, June, pp. 759-766, 1988.

[3] Higashimura, M., Current-Mode Allpass Filter Using FTFN with Grounded Capacitor, Electron. Lett., vol.27, no.13, June, pp. 1182-1183, 1991.

[4] Comer, D.T., Comer, D.J. and Gonzales, J.R., A High-Frequency Integrable Bandpass Filter Configuration, IEEE Transactions on Circuits and Systems-II: Analog and Digital Signal Processing, vol. 44, no.10, October, pp. 856-861, 1997.

[5] Pookaiyaudom, S. and Mahattanakul, J., A 3.3-Volt High-Frequency Capacitorless Electronically-Tunable Log-Domain Oscillator, Proceedings of the 1995 IEEE International Symposium on Circuits and Systems, ISCAS'95, vol.2, pp. 829-832, 1995.

[6] Tang, J. D. v.d. and Kasperkovitz, D., A 0.9-2.2 GHz Monolithic Quadrature Mixer Oscillator for Direct-Conversion Satellite Receivers, Proceedings of the IEEE International Solid-State Circuits Conference, pp. 88-89, 1997.

[7] Nagasawa, T. Hyogo, A. and Sekine, K., A 2V-500MHz CMOS Continuous-Time Current-Mode Filter using the Gate-Source Capacitance of the MOSFET, ISPACS'99, pp. 493-496, 1999.

[8] Toumazou, C., Hughes, J.B. and Battersby, N.C. (ed.) Switched-Currents an Analogue Technique for Digital Technology, IEE Circuits and Systems Series 5, Short Run Press, Ltd., Exeter, UK, 1993.

[9] Sedra, A.S. and Smith, K.C., Microelectronic Circuits, Oxford University Press, p. 445, 1998.

[10] Baker, R. J., Li, H.W. and Boyce, D.E., CMOS Circuit Design, Layout and Simulation, IEEE Press, U.S.A., p. 174, 1998.

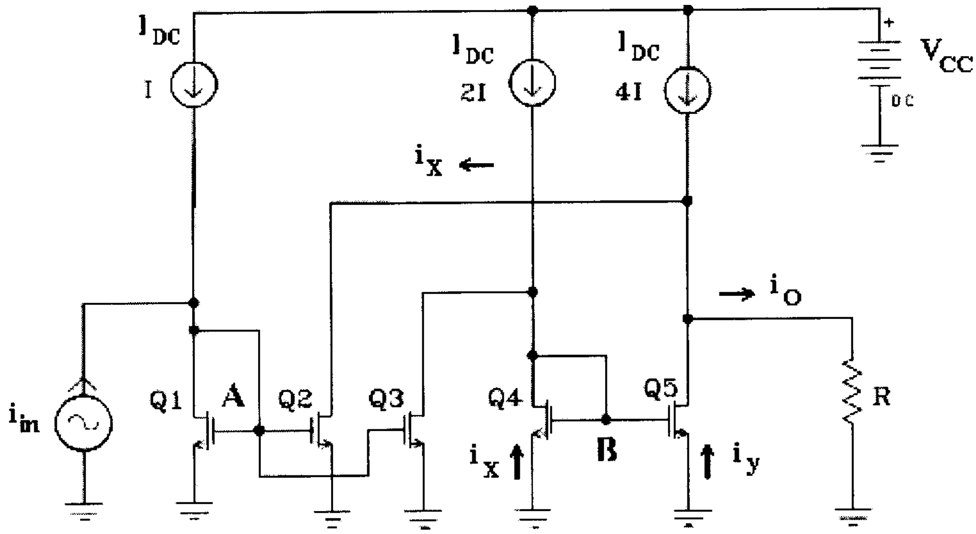

Figure 1 : Schematic diagram of the CMOS capacitorless current-tunable all-pass filter.

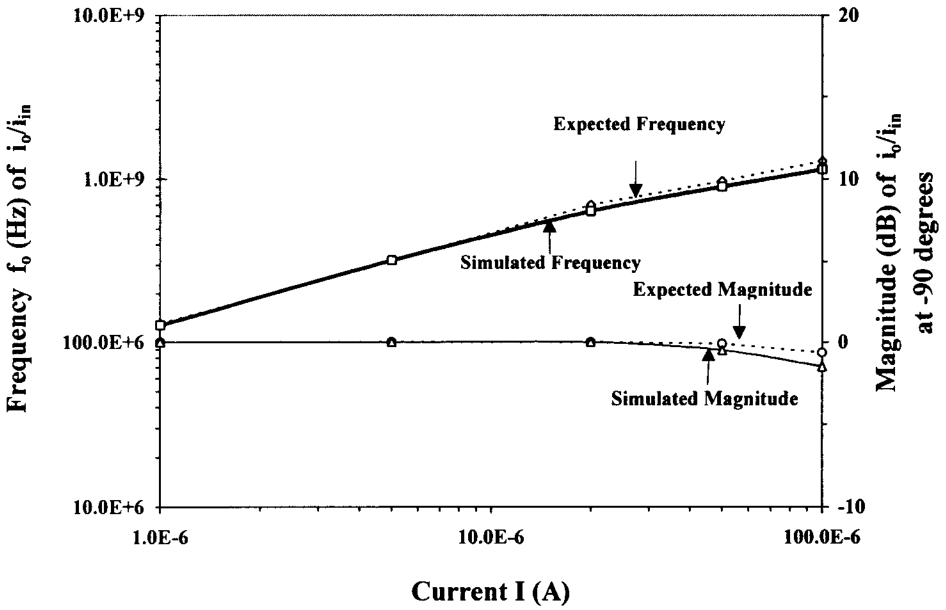

Figure 2 : Frequency f_o (Hz) and magnitude M (dB) at $\phi = -90°$ versus I where the aspect ratios of Q4 and Q5 are, for the first case ($\tau_a << \tau_b$), 16W/L and 32W/L, respectively.

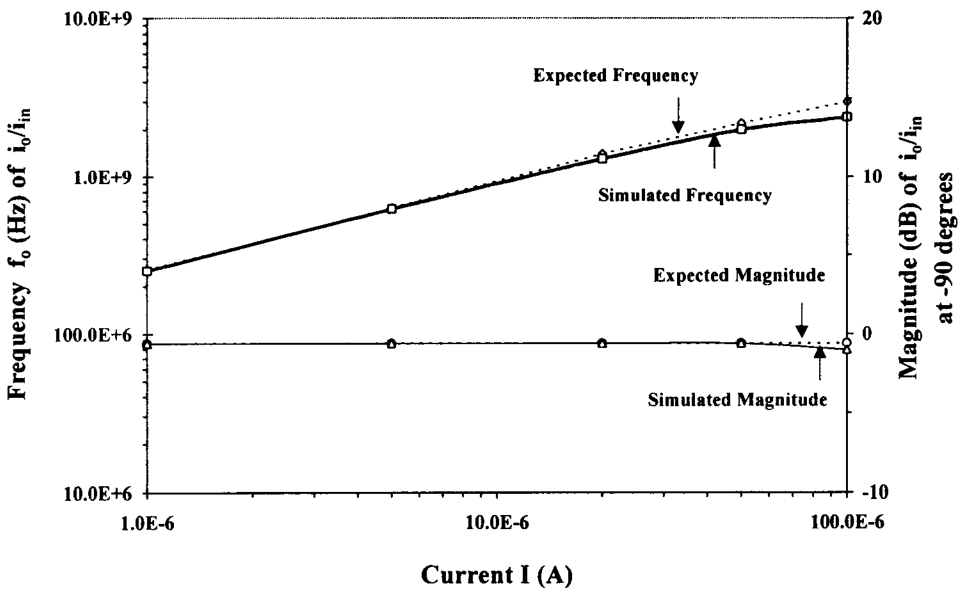

Figure 3 : Frequency f_o (Hz) and magnitude M (dB) at $\phi = -90°$ versus I where the aspect ratios of Q4 and Q5 are, for the second case ($\tau_a < \tau_b$), 2W/L and 4W/L, respectively.

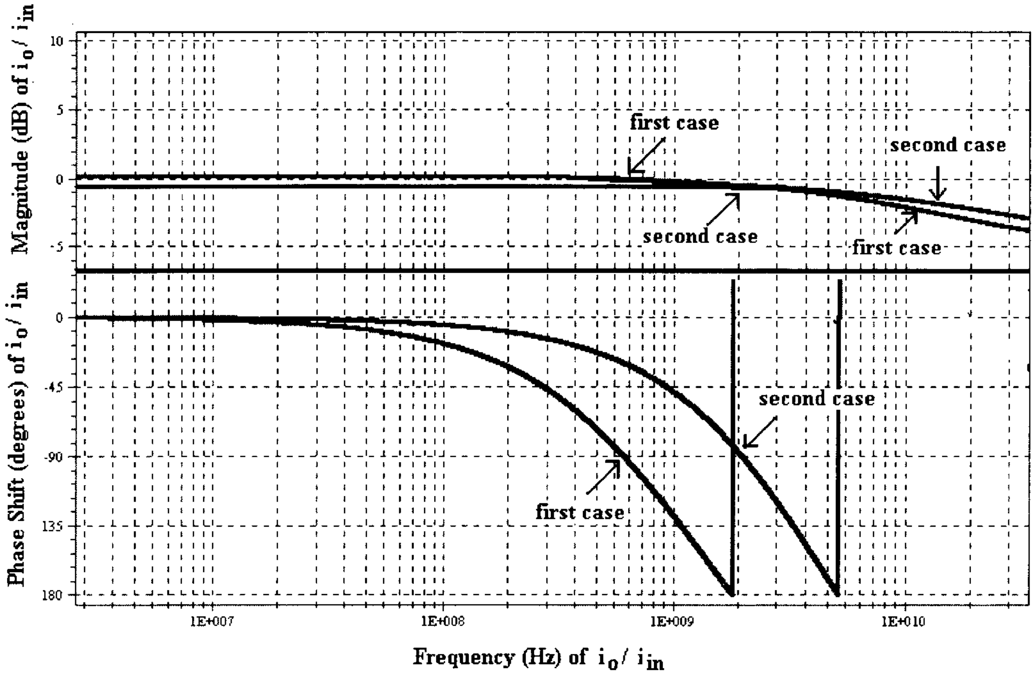

Figure 4 : Magnitude (dB) and phase shift (degrees) of (6) and (3) versus frequency (Hz) at I = 20 uA and 50 uA for the first case ($\tau_a << \tau_b$) and the second case ($\tau_a < \tau_b$), respectively.